JTE HCM-UTE
ISSN: 2615-9740
JOURNAL OF TECHNICAL EDUCATION SCIENCE
Ho Chi Minh City University of Technology and Engineering
Website: https://jte.edu.vn
Email: jte@hcmute.edu.vn

Forecast-Guided Economic Dispatch of BESS in Grid-Export-Only PV Systems

Gia Tue Tang, Mi Sa Nguyen Thi, Phuong Nam Tran, Dinh Nhon Truong*
Ho Chi Minh City University of Technology and Engineering, Vietnam
*Corresponding author. Email: nhontd@hcmute.edu.vn

ARTICLE INFO

Received:	03/12/2025
Revised:	03/03/2026
Accepted:	22/06/2026
Online First:	19/08/2026
Published:	

KEYWORDS

Photovoltaic forecasting;
Battery Energy Storage System (BESS);
Techno-economic analysis;
Tariff structure impact;
Gradient Boosted Trees forecasting.

ABSTRACT

High short-term variability in photovoltaic (PV) output causes inverter clipping, curtailment, and revenue loss in grid-export-only solar plants. This paper presents a forecast-guided operational framework that integrates an hour-ahead Gradient Boosted Trees (GBT) model with a receding-horizon mixed-integer linear programming (MILP) dispatch strategy for Battery Energy Storage Systems (BESS). A dataset of 30,579 hourly samples, combining NASA POWER meteorological variables and AC-side PV measurements from March 2022 to July 2024, is used to train and evaluate the forecasting model. The GBT achieves strong performance with a normalized RMSE of 0.152 (per-unit scale) and a MAPE of 6.65%. These forecasts drive the MILP scheduler, which incorporates inverter limits, state-of-charge dynamics, non-simultaneous charge/discharge constraints, and throughput-based degradation. A techno-economic comparison of BESS capacities from 250 to 1,000 kWh under fixed PPA and Time-of-Use tariffs shows that all capacities ≥ 250 kWh fully eliminate curtailment, while the TOU–750 kWh configuration maximizes economic returns. The results highlight the importance of moderate BESS sizing for cost-effective deployment in grid-export-only PV systems.

DOI: https://doi.org/10.54644/jte.2026.2046

1. Introduction

The rapid growth of renewable energy has positioned photovoltaic (PV) systems as a key contributor to modern power networks. However, the intermittency of solar generation creates operational challenges such as grid congestion, curtailment, and unstable export profiles. Accurate short-term forecasting and optimization-driven scheduling are essential to mitigate these issues.

Recent research on PV forecasting has highlighted the effectiveness of artificial intelligence (AI) and machine learning techniques over conventional methods. A recent review of solar forecasting developments highlighted AI as a promising approach [1]. A comparison of AI with statistical and physical models [2] revealed that statistical methods such as linear regression often lack adaptability to complex patterns. At the same time, physical models require precise meteorological data, making them less feasible for long-term forecasting. Stochastic and Markov-based models were utilized to quantify PV uncertainty, but encountered challenges in handling large-scale, nonlinear datasets [3].

Machine learning and deep learning models have been widely applied to address these challenges. Several ML algorithms, including artificial neural networks (ANN), support vector machines (SVM), random forest (RF), and XGBoost, were applied for solar power forecasting in [4]. ANN has the best prediction accuracy out of all of these. Nonetheless, this result showed a moderate level of prediction accuracy, with an MAE of 9.913 kW and an RMSE of 13.447 kW for PV output prediction. Other studies employed models such as multilayer perceptron neural networks (MLPNN), convolutional neural networks (CNN), and k-nearest neighbors (kNN) [5], as well as hybrid models like LSTM-Copula [6] and LSTM-RNN [7], demonstrating improved performance in both short- and medium-term forecasting. Deep learning methods have also been applied for hour-ahead solar irradiance forecasting using cloud image analysis [8]. This study showed great accuracy in capturing irradiance changes, with a normalized root mean squared error (nRMSE) of 7.98%.

Battery operation has become a key mechanism for balancing intermittent PV generation with fluctuating grid export conditions. To mitigate the volatility of solar output, recent studies have increasingly integrated PV forecasts into optimization-based control frameworks for battery energy storage systems (BESS).

A fuzzy logic–based control strategy combined with the Jellyfish Optimization Algorithm was developed to manage battery charging in PV systems [9]. By utilizing forecasted solar irradiance, their approach adaptively tuned PI controller parameters, leading to improved charging performance and greater robustness against weather-induced variability. Furthermore, a Dual-Self Adaptive Algorithm was introduced to optimize charge–discharge behavior in DC substation batteries [10]. Expanding on the resilience dimension, the relevance of resilience-oriented BESS operation within PV–battery integrated systems was highlighted in [11]. Similarly, integrating PV forecasting into the multi-objective optimization of storage operation for renewable-dominant microgrids has been shown to simultaneously minimize operational costs, ensure reliability, and mitigate degradation effects [12].

Nevertheless, most existing work focuses on systems with local loads or assumes deterministic forecasts, with limited attention to grid-export-only PV plants under tariff-based markets. In grid-export-only PV plants, all generated energy is sold directly to the grid, and thus electricity tariffs and market rules critically affect system operation. Few prior studies have examined battery dispatch in such tariff-driven export-only contexts. This work fills that gap by developing a forecast-driven optimization framework that integrates high-resolution PV forecasts and satellite-derived meteorological features with tariff-driven, MILP-based economic dispatch. The contributions are threefold: (i) development of a high-resolution PV forecasting model, (ii) formulation of a complete MILP dispatch incorporating inverter and degradation constraints, and (iii) techno-economic evaluation of BESS capacities under PPA and TOU tariffs.

2. Methodology

2.1. PV Forecasting Layer

Meteorological variables from NASA POWER [13] and measured AC-side PV output (March 2022–July 2024) were preprocessed to handle missing values and normalized via Min-Max scaling. Engineered features, including lagged PV outputs and seasonal indicators, were added to capture temporal dependencies. A Gradient Boosted Trees (GBT) model was employed for hour-ahead forecasting due to its proven robustness in handling nonlinear meteorological interactions. The dataset was chronologically split into training (March 2022–December 2023), validation (January–June 2024), and testing (July 2024). The complete data processing and GBT forecasting pipeline is executed as a sequential workflow, as illustrated in Figure 1.

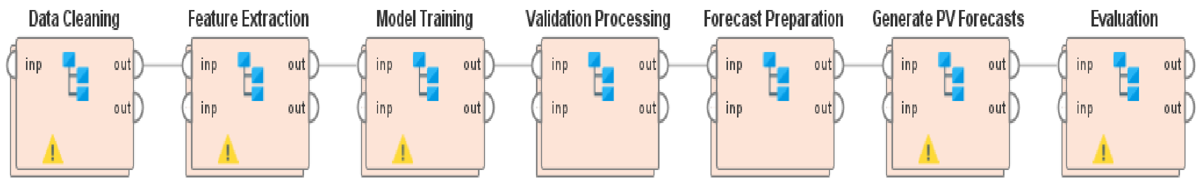

Figure 1. *AI model-based Gradient Boosted Trees.*

2.2. Forecast-Driven Economic Optimization Layer for PV-BESS Systems

This layer determines optimal BESS scheduling based on PV forecasts while accounting for tariff schemes, degradation, and curtailment. The objective is to maximize economic returns while maintaining operational feasibility.

2.2.1. Objective function

The optimization problem aims to determine the optimal charge/discharge schedule of the BESS that maximizes long-term economic benefits while minimizing degradation-induced losses.

Equation (1) defines the combined objective function, balancing energy revenue and degradation cost through weighting coefficients α and β.

$$\max J = \alpha J_{\text{energy}} - \beta J_{\text{degr}} \tag{1}$$

The weighting coefficients α and β balance the trade-off between short-term profit and long-term battery lifespan. In this study, the weighting coefficients are set to $\alpha = 1$ and $\beta = 1$, placing equal economic weight on revenue generation and battery wear penalties.

The economic component J_{energy} represents the net revenue obtained from PV energy exported to the grid in Equation (2).

$$J_{energy} = \sum_{t=1}^{H} \left(\pi_t P_t^{\exp} \right) \Delta t \tag{2}$$

In the fixed-price PPA scenarios, π_t remains constant throughout the operation period. In TOU-based scenarios, π_t varies according to the time-of-use tariff schedule, encouraging the optimizer to store energy during off-peak hours and discharge at peak prices for arbitrage gains.

To quantitatively represent battery aging within the optimization framework, a composite degradation cost function is employed as Equation (3).

$$J_{\deg r} = \sum_{t=1}^{H} \left(c_1 \left| P_t^{char} \right| + c_2 \left| P_t^{dis} \right| \right) \cdot \Delta t \tag{3}$$

where c_1, c_2 are charge- and discharge-related wear coefficients. This formulation penalizes aggressive cycling that would shorten battery lifetime. In the optimization stage, the degradation coefficients c_1 and c_2 are set to a small value (totaling 0.01 VND/kWh) to serve as a soft mathematical penalty. This prevents the MILP solver from engaging in unrealistic micro-cycling while maintaining computational focus on revenue maximization. The actual economic depreciation is subsequently handled in the techno-economic post-processing phase. Battery aging is represented using a linear throughput-based degradation model. In this approach, battery wear is assumed to be proportional to the total energy processed through the battery. Accordingly, each unit of energy processed by the battery (either charging or discharging) incurs a marginal degradation cost, which reflects the economic impact of battery wear over time. This simplified formulation introduces an economic penalty for excessive cycling while maintaining computational efficiency within the MILP optimization framework.

The rolling-horizon (RH) mechanism executes the MILP-based dispatch iteratively, using updated PV forecasts to generate optimal charge/discharge decisions over a look-ahead window. Only the first control action is applied to the physical system, ensuring adaptability to forecast errors and short-term variability. The accumulated operational outcomes—including energy exported, curtailed power, battery throughput, and degradation cost—are then used to compute the economic performance of the system under different tariff schemes and battery capacities.

2.2.2. Power balance, export and curtailment

At each hourly step *t*, the relationship between PV generation, battery operation, and grid export is represented by Equation (4).

$$P_t^{exp} = P_t^{PV} + P_t^{dis} - P_t^{char} - P_t^{curt} \tag{4}$$

Here, $P_t^{\exp}$ denotes the AC power actually exported to the grid (measured at the point of connection under the PPA contract). P_t^{PV} represents the total AC power output of the PV inverter, P_t^{dis} and P_t^{char} are the discharging and charging power of the BESS, respectively, and P_t^{curt} accounts for curtailed power due to inverter limits or operational constraints. This formulation assumes grid-export-only operation (no power import), where the BESS can only charge from PV surplus energy.

2.2.3. Battery dynamics

The dynamic behavior of the battery is represented through its state-of-charge (SOC) trajectory, which reflects the effects of charging and discharging operations. Equation (5) describes the state-of-charge evolution of the battery, accounting for charging/discharging efficiencies and nominal capacity.

$$SOC_t = SOC_{t-1} + \frac{\left(\eta^{char} P_t^{char} - \dfrac{P_t^{dis}}{\eta^{dis}}\right) \cdot \Delta t}{E_{batt}} \times 100\% \tag{5}$$

Here, η^{char} and η^{dis} denote charging and discharging efficiencies, respectively. The initial state of charge ($SOC_{t=0}$) at the beginning of the simulation horizon is set to 50%. At each hourly time step, the optimization model is solved using the one-hour-ahead PV generation forecast, after which only the first-hour BESS dispatch decision is implemented before the optimization is repeated for the next time step.

2.2.4. Operational constraints

Equations (6)–(9) impose operational constraints, including inverter conversion limits, maximum charge/discharge power, and SOC bounds:

$$0 \le P_t^{\exp} \le P^{AC,\max} \tag{6}$$

$$0 \le C_t \le P_t^{PV} \tag{7}$$

$$0 \le P_t^{char} \le P^{char,\max},\ 0 \le P_t^{dis} \le P^{dis,\max} \tag{8}$$

$$SOC^{\min} \le SOC_t \le SOC^{\max} \tag{9}$$

Here, $P^{AC,\max}$ is the total AC conversion capacity of installed inverters (600 kW in the case study), $P^{char,\max}$ and $P^{dis,\max}$ are the BESS power limits, and the SOC bounds are set according to manufacturer recommendations.

To prevent simultaneous charging and discharging, we introduce a binary decision variable $z_t \in \{0, 1\}$ in Equation (10), which transforms the problem into a MILP. The variable controls mutually exclusive operations via on/off constraints.

$$P_t^{char} \le z_t P^{char,\max},\ P_t^{dis} \le (1-z_t) P^{dis,\max} \tag{10}$$

2.3. Evaluation Metrics

2.3.1. Economic Performance Evaluation

Base revenue represents the annual income obtained from exporting PV energy to the grid without a battery. It is computed as J_{energy}.

Arbitrage Savings quantifies BESS integration by reflecting how effectively the battery exploits TOU price differences to increase financial returns:

$$Arbitrage\,Savings = \sum_{t=1}^{H}\left(\pi_t P_t^{\exp,withBESS}\right)\cdot \Delta t - \sum_{t=1}^{H}\left(\pi_t P_t^{\exp,noBESS}\right)\cdot \Delta t \tag{11}$$

Here, Δt is the time step resolution (1 hour), P_t^{exp} is in kW, and π_t is the electricity tariff in VND/kWh. The total net financial gain from the BESS is defined as *TotalNetBenefit*.

The simple payback period is calculated as:

$$Payback = \frac{CAPEX_{BESS}}{TotalNetBenefit} \tag{12}$$

The net present value (NPV) over an N-year horizon with discount rate r is:

$$NPV = \sum_{y=1}^{N} \frac{TotalNetBenefit}{(1+r)^y} - CAPEX_{BESS} \tag{13}$$

2.3.2. Operational Performance Metrics

Operationally, Curtailment Reduction and Estimated Battery Aging Rate are defined by Equations (14) and (15):

$$Curtailment\ Reduction = \frac{\sum_{t=1}^{T} (P_t^{curt,base} - P_t^{curt,BESS}) \cdot \Delta t}{\sum_{t=1}^{T} P_t^{curt,base} \cdot \Delta t} \times 100\% \tag{14}$$

$$Estimated\ Battery\ Aging\ Rate = \frac{\sum_{t=1}^{T} P_t^{dis} \cdot \Delta t}{E_{batt} \times 80\% \times 5000} \times 100\% \tag{15}$$

Here, E_{batt} is the installed battery energy capacity (in kWh), P_t^{dis} is the discharge power (in kW), and Δt is the time step (1 hour). Here, T denotes the total hours in the simulation horizon (e.g. $T = 21168$ for March 2022–July 2024). To convert totals into per-year values, we use the factor 8760 h/year.

2.4. Case study

2.4.1. PV System Description

The case study investigates a grid-connected solar PV installation located in Binh Duong Province, Vietnam. The PV array comprises 1,620 Canadian Solar modules, each rated at 445 Wp, yielding a total DC capacity of 720.9 kWp. The system is interfaced with the grid via six Sungrow inverters, each rated at 100 kW (model series A200926), providing an aggregate AC capacity of 600 kW. This design results in a DC/AC ratio of 1.2, a common practice that maximizes inverter utilization under varying irradiance conditions.

2.4.2. BESS Description and Selection

To enable a comparative assessment of technical and economic performance, the battery energy storage system (BESS) is modeled as a lithium iron phosphate (LFP) unit with multiple candidate capacities ranging from 250 kWh to 1000 kWh. All configurations follow a consistent set of electrical and operational constraints, including a 0.5C power rating, state-of-charge (SOC) limits of 10–90%, and charge and discharge efficiencies of 95% per direction. These parameters are representative of commercially available industrial BESS solutions and ensure that each tested capacity can be realistically deployed alongside the PV system. The technical specifications used for all simulated BESS configurations are summarized in Table 1.

From an economic perspective, a detailed cost structure is incorporated to ensure that the optimization outcomes reflect realistic deployment conditions. The CAPEX of the BESS is explicitly scaled with system size, at 12 million VND/kWh for 250 kWh, 10 million VND/kWh for 535 kWh, 8 million VND/kWh for 750 kWh, and 6 million VND/kWh for 1000 kWh. A fixed balance-of-system cost of 10 million VND is uniformly applied. Annual O&M expenses are assumed to be 3% of the initial CAPEX.

Table 1. *BESS parameters.*

Parameter	Value	Unit	Notes
Technology	Lithium iron phosphate	-	LFP, commercial system
Nominal energy capacity	250-1000	kWh	Two cases
Charge/discharge efficiency	95	%	Applied per direction
SOC operating limits	10–90	%	Lifetime-preserving operating window
Lifetime model	>5000 cycles; cycle + SOC based	-	Based on reported LFP battery cycle life [14]

2.4.3. Time-of-Use (TOU) Tariff Framework

The Time-of-Use (TOU) tariff values are adapted for simulation purposes. Three periods are defined: off-peak, normal, and peak hours, as summarized in Table 2.

Under the TOU scenario, the BESS schedules its operation to store energy during off-peak periods and export during high-price hours to maximize profit. For comparison, the fixed-price PPA scenario assumes a constant tariff of 1400 VND/kWh.

Table 2. *TOU tariff schedule used in the market scenarios (VND/kWh).*

Period	Time range	Tariff (VND/kWh)	Description
Off-peak	22:00–04:00	1000	Lowest demand, low selling price
Normal	04:00–09:00, 17:00–22:00	1800	Regular operation period
Peak	09:00–17:00	3000	Highest demand, maximum selling price

It is important to note that the TOU schedule adopted in this study does not represent the standard national retail tariff, which typically features an evening peak driven by residential demand. Instead, it simulates a Corporate Power Purchase Agreement (CPPA) or Direct PPA (DPPA) pricing structure tailored for Commercial and Industrial (C&I) off-takers in major industrial hubs like Binh Duong Province. In such manufacturing hubs, the energy demand is heavily dominated by daytime factory operations, heavy machinery, and intensive HVAC (cooling) loads, creating a continuous peak from 09:00 to 17:00. This customized tariff structure is strategically designed to incentivize the PV-BESS system to dispatch stored energy during these high-stress daytime hours, perfectly matching the local corporate load profile.

The methodological framework described above integrates forecasting, optimization, and rolling-horizon execution into a unified process. To consolidate these elements, Figure 2 presents the conceptual workflow of the PV–BESS system. The workflow begins with data preprocessing, where outliers are removed and the dataset is divided into training, validation, and testing subsets to ensure data quality and model reliability. Feature engineering is then applied to capture the temporal characteristics of PV generation, including lagged PV outputs (t–1 to t–24) and autocorrelation features, while meteorological variables are normalized. The processed data are used to train a Gradient Boosted Trees (GBT) model for hour-ahead PV power prediction. If the forecasting performance satisfies the predefined accuracy threshold (MAPE $\leq$ 10%), the predicted PV output is subsequently used as an input to the MILP-based dispatch model. The optimization module evaluates multiple BESS capacities under the given tariff structures and determines the optimal scheduling strategy. Finally, the techno-economic evaluation identifies the battery capacity that provides the highest economic performance based on metrics such as revenue, net benefit, NPV, and payback period, while also assessing technical indicators including curtailment reduction and PV utilization.

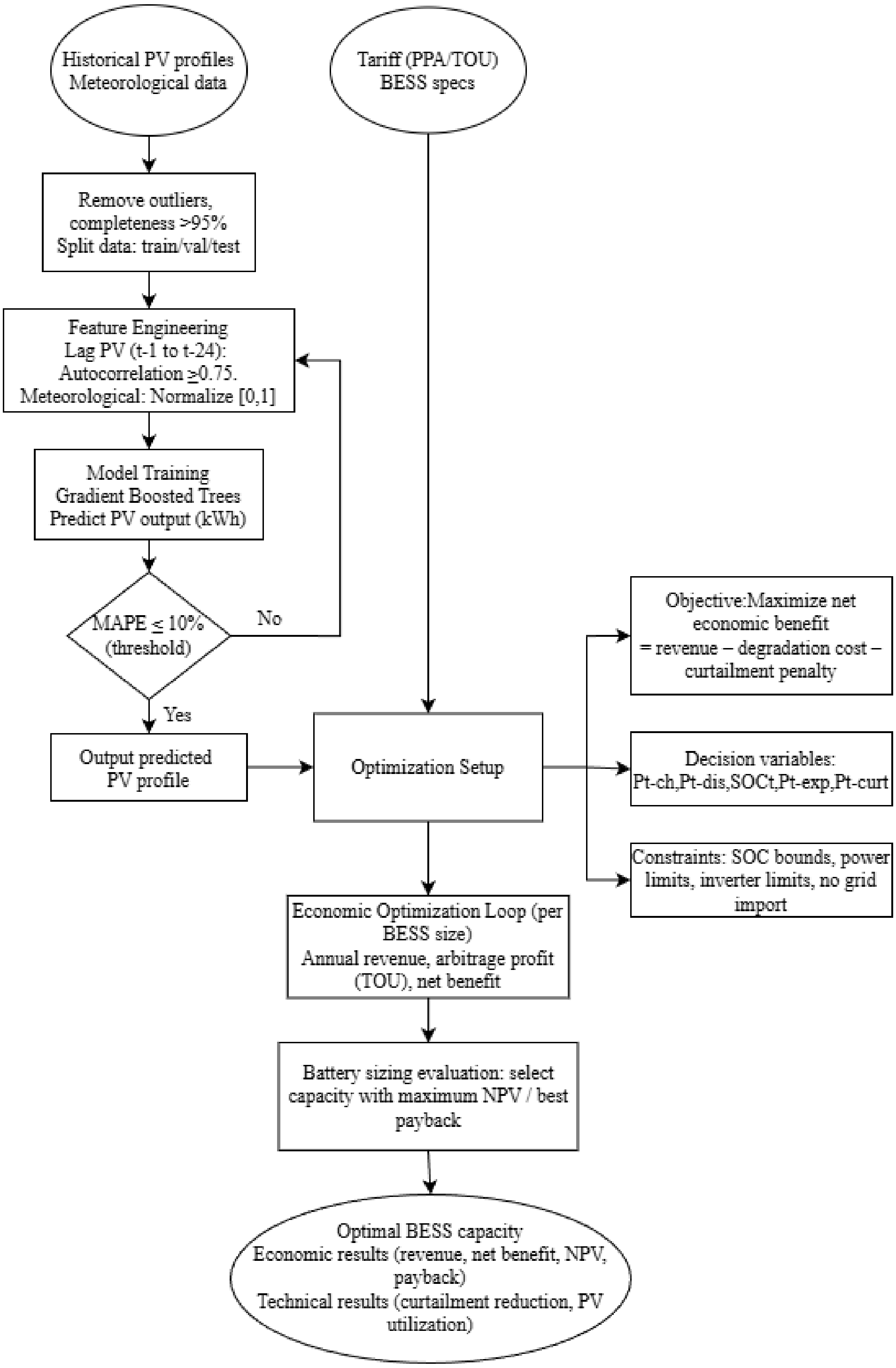

Figure 2. *Conceptual workflow of the PV-BESS forecasting and optimization framework.*

3. Results

3.1. Forecasting performance

The GBT model demonstrates strong predictive performance on the test set, achieving a normalized RMSE of 0.152 (on a 0–1 scale) and a MAPE of 6.65%. The low normalized error (0.152) indicates negligible point forecast deviations relative to the plant's rated capacity, while the MAPE (6.65%) confirms high percentage accuracy despite the inherent variability of cloud motion. This high accuracy is visually confirmed in Figure 3, which demonstrates that the predicted PV output closely tracks the actual generation profile throughout the testing period.

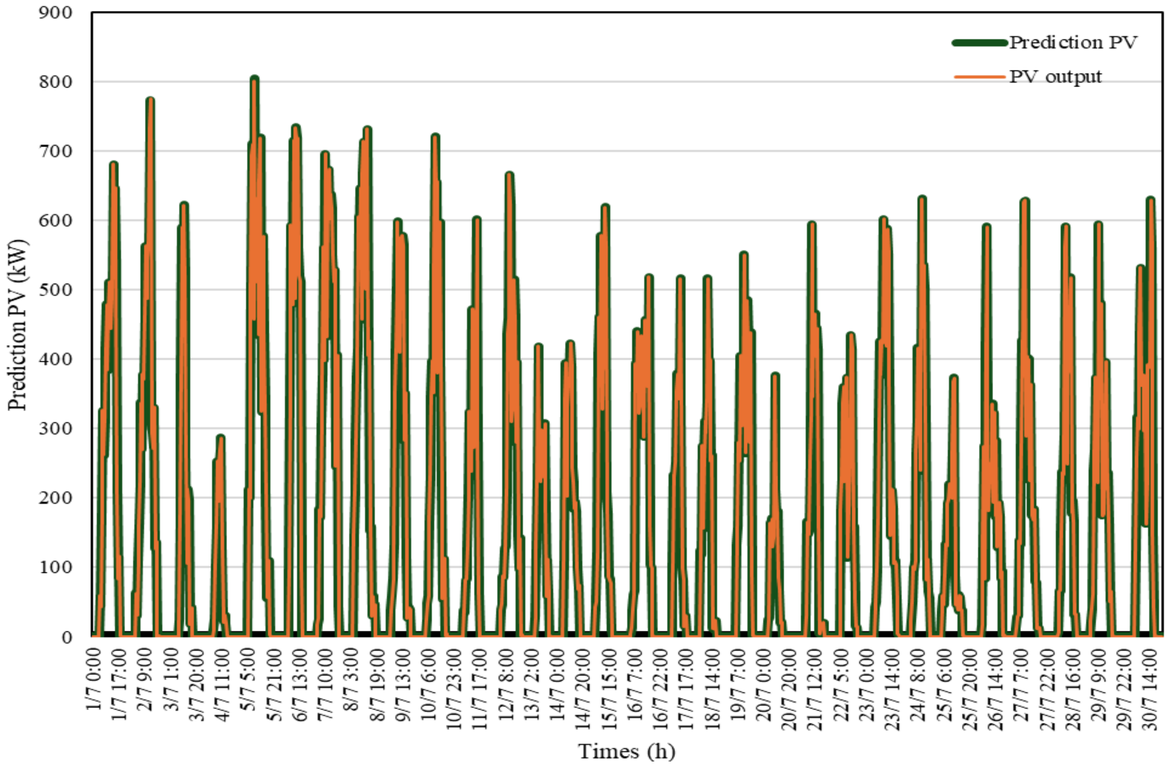

***Figure 3**. Comparison of Predicted and Actual PV Output (Test Data, July 2024).*

3.2. Scenario comparison

For each tested BESS capacity, the optimization was executed over a full-year time series, after which technical indicators (curtailment, SOC profile, utilization rate) and economic metrics (annual revenue, arbitrage gains, net benefit, payback period, and NPV) were calculated directly from the resulting dispatch profiles. Aggregate performance results for all scenarios are presented in Tables 3 and 4. It should be noted that the optimization may schedule multiple partial charge–discharge events within a day depending on PV availability and export constraints. Therefore, the reported battery activity reflects total energy throughput rather than an equivalent number of full charge–discharge cycles.

***Table 3.** Economic Indicators for All Scenarios.*

Scenario	Base Revenue (VND/year)	Arbitrage Savings (VND/year)	Total Net Benefit (VND/year)	Payback (years)	NPV (VND)
No BESS	1.67E+09	0	0		0
TOU – 250 kWh	1.42E+09	2.02E+09	1.66E+09	1.8	8.63E+09
TOU – 535 kWh	1.42E+09	3.88E+09	3.24E+09	1.7	1.74E+10
TOU – 750 kWh	1.42E+09	5.17E+09	4.44E+09	1.4	2.52E+10
TOU – 1000 kWh	1.42E+09	2.17E+09	1.45E+09	4.1	4.16E+09
PPA – 250 kWh	1.67E+09	1.72E+09	1.36E+09	2.2	6.52E+09
PPA – 535 kWh	1.67E+09	3.17E+09	2.52E+09	2.1	1.23E+10
PPA – 750 kWh	1.67E+09	4.12E+09	3.39E+09	1.8	1.78E+10
PPA – 1000 kWh	1.67E+09	1.72E+09	9.88E+08	6.1	9.42E+08

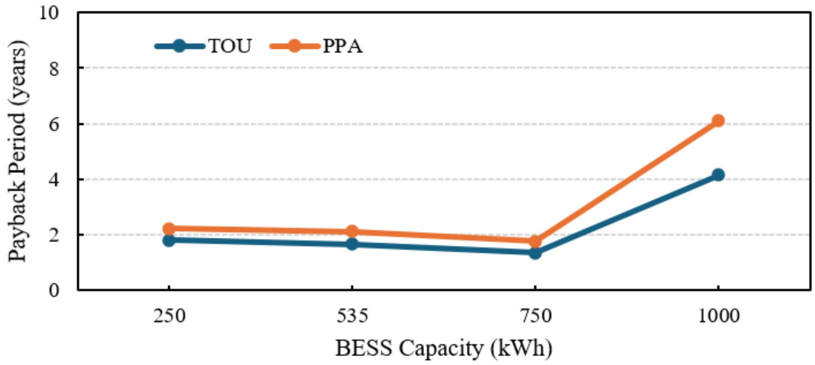

Figure 4. *Payback period versus BESS capacity under TOU and fixed PPA tariffs.*

Figure 4 illustrates how the payback period varies as a function of BESS capacity under both the fixed PPA and TOU tariff structures. The TOU scenario consistently achieves shorter payback periods for medium-sized batteries (250–750 kWh), reaching its minimum value of 1.4 years at 750 kWh. Beyond 750 kWh, however, the payback period rises significantly as the marginal economic benefit of additional storage declines and the battery becomes increasingly under-utilized. In contrast, the fixed-price PPA case exhibits longer payback periods that increase sharply to 6.1 years at 1000 kWh, indicating limited price-driven arbitrage opportunities to offset the high capital cost of oversized batteries. Overall, the figure demonstrates the strong influence of tariff mechanisms on storage profitability and highlights the need for size-specific optimization in grid-export PV systems. All BESS-integrated scenarios eliminate PV curtailment, with capacities ≥250 kWh fully absorbing excess generation under the studied C&I profile. While previous findings suggest moderate BESS sizing (15–25% of PV capacity) is typically sufficient to remove curtailment [4], this case study required a larger fraction (~35% of the 720.9 kWp DC capacity) to fully absorb excess generation, directly reflecting the plant's DC/AC ratio and strict export constraints.

Table 4. *Operational Indicators for All Scenarios.*

Scenario	Curtailment Reduction (%)	Average SOC (%)	Estimated Battery Aging Rate (%)
No BESS	0.0	-	-
PPA – 250 kWh	100.0	12.4	9.1
TOU – 250 kWh	100.0	13.1	9.1
PPA – 535 kWh	100.0	14.5	6.8
TOU – 535 kWh	100.0	15.2	7.4
PPA – 750 kWh	100.0	16.8	5.2
TOU – 750 kWh	100.0	17.5	6.1
PPA – 1000 kWh	100.0	22.4	3.9
TOU – 1000 kWh	100.0	32.2	4.8

While curtailment is entirely resolved, overall economic viability remains heavily dependent on the tariff. As detailed in Tables 3 and 4, TOU pricing consistently outperforms the fixed PPA by leveraging midday surplus for peak-hour arbitrage. The TOU–750 kWh configuration emerges as optimal, maximizing NPV (25.2 billion VND) and arbitrage savings (5.17 billion VND/year) with a rapid 1.4-year payback. Conversely, oversized configurations (1000 kWh) yield diminishing marginal returns, evidenced by significantly reduced physical aging rates (3.9–4.8%) and elevated average SOC due to severe under-utilization, matching patterns reported in recent studies [11], [15].

4. Discussion

The analyzed PV plant has a DC capacity of 720.9 kWp and an AC export limit of 600 kW, corresponding to a DC/AC ratio of 1.2. During high-irradiance periods, this configuration generates surplus energy that cannot be fully exported due to inverter clipping, making battery storage integration a technically valuable enhancement. Simulation results indicate that a minimum battery capacity of 250 kWh is sufficient to eliminate curtailment across the operating year, while also enabling grid-price arbitrage under TOU tariff conditions.

For this system scale, the optimal BESS size is identified near 750 kWh (≈1.0 kWh per kWp or 1.25 hours at full AC rating), which delivers the highest economic returns and shortest payback periods. At this capacity, the BESS can reliably shift approximately 600 kW of curtailed or low-price off-peak energy into peak periods, thereby maximizing revenue while maintaining low average state of charge and high utilization. At 1000 kWh, marginal economic benefits decline sharply due to reduced cycling depth and under-utilized capacity, indicating oversizing relative to the PV generation profile. Based on these findings, Table 5 summarizes the practical implications and recommended BESS sizing for various deployment scenarios.

Table 5. *Practical implications for deployment.*

Intended Use Case	Recommended BESS Size (for this PV system)	Operational Benefit
Residential clusters / small micro grids	250–400 kWh	Eliminates clipping losses, supports evening load, reduces curtailed energy loss
Commercial & Industrial (C&I) facilities	500–750 kWh (optimal ≈ 750 kWh)	Maximizes TOU price arbitrage, reduces peak demand charge, enables backup capability
Export-focused / grid services (V2G, FFR, AGC)	750–1000 kWh	Higher flexibility for ancillary services, but reduced financial efficiency beyond 750 kWh

This level of capability is particularly suitable for manufacturing zones in Binh Duong province and Southern Vietnam, where load profiles exhibit a sustained daytime peak and tariff structures differ significantly between daytime and evening periods. Overall, this study demonstrates that forecast-guided economic dispatch can simultaneously eliminate PV curtailment and enhance financial viability in grid-export-only solar plants. The findings highlight the importance of moderate BESS sizing, particularly around 750 kWh, to balance technical reliability and economic efficiency. Future work will extend the framework to multi-site PV portfolios and incorporate probabilistic forecasts to address uncertainty under dynamic tariff structures.

5. Conclusion

This paper validates a forecast-driven dispatch framework for grid-export-only PV plants, coupling an hour-ahead Gradient Boosted Trees predictor with a receding-horizon MILP scheduler to eliminate curtailment and enable profitable TOU arbitrage. Techno-economic simulations identify a 750 kWh BESS (≈1.0 kWh/kWp) as the optimal configuration that maximizes net present value, whereas the largest tested capacity (1000 kWh) already shows under-utilization and poorer payback, suggesting further oversizing would perform worse still. These results highlight that combining accurate short-term forecasting with moderate, workload-matched sizing is crucial for maximizing BESS value in export-only setups. Finally, future work will address current limitations—namely, linear degradation proxies and fixed tariff scenarios—by integrating probabilistic forecasting, detailed cell-level aging models, and dynamic market participation.

Conflict of Interest

The authors declare that there is no conflict of interest regarding the publication of this paper.

REFERENCES

[1] N. Rahimi *et al.*, “A Comprehensive Review on Ensemble Solar Power Forecasting Algorithms,” *Journal of Electrical Engineering and Technology*, vol. 18, no. 2, pp. 719–733, 2023, doi: 10.1007/s42835-023-01378-2.

[2] F. Nicoletti and P. Bevilacqua, "Hourly Photovoltaic Production Prediction Using Numerical Weather Data and Neural Networks for Solar Energy Decision Support," *Energies (Basel).*, vol. 17, no. 2, 2024, doi: 10.3390/en17020466.

[3] W. Hansong, L. Xiangchao, L. Hang, and R. Xulin, "Optimal Allocation of Photovoltaic &Energy Storage Grid System Based on Markov Chain," *Proceedings - 2021 3rd International Conference on Applied Machine Learning, ICAML 2021*, pp. 471–476, 2021, doi: 10.1109/ICAML54311.2021.00105.

[4] Y. Ledmaoui, A. El Fahli, A. Elmaghraoui, M. El Aroussi, R. Saadane, and A. Chehri, "Machine Learning Techniques Using the Rapid Miner Tool for Solar Production Forecasting," *Proceedings - 2023 International Conference on Digital Age and Technological Advances for Sustainable Development, ICDATA 2023*, no. May, pp. 120–125, 2023, doi: 10.1109/ICDATA58816.2023.00030.

[5] A. Mellit, A. Massi Pavan, and V. Lughi, "Short-term forecasting of power production in a large-scale photovoltaic plant," *Solar Energy*, vol. 105, pp. 401–413, Jul. 2014, doi: 10.1016/J.SOLENER.2014.03.018.

[6] S. Han, Y. H. Qiao, J. Yan, Y. Q. Liu, L. Li, and Z. Wang, "Mid-to-long term wind and photovoltaic power generation prediction based on copula function and long short term memory network," *Appl. Energy*, vol. 239, pp. 181–191, Apr. 2019, doi: 10.1016/J.APENERGY.2019.01.193.

[7] M. Abdel-Nasser and K. Mahmoud, "Accurate photovoltaic power forecasting models using deep LSTM-RNN," *Neural Comput. Appl.*, vol. 31, no. 7, pp. 2727–2740, Jul. 2019, doi: 10.1007/S00521-017-3225-Z/METRICS.

[8] R. A. Rajagukguk, R. Kamil, and H. J. Lee, "A deep learning model to forecast solar irradiance using a sky camera," *Applied Sciences (Switzerland)*, vol. 11, no. 11, 2021, doi: 10.3390/app11115049.

[9] R. Ahmed Ali Agoub, A. Hançerlioğullari, J. Rahebi, and J. M. Lopez-Guede, "Battery Charge Control in Solar Photovoltaic Systems Based on Fuzzy Logic and Jellyfish Optimization Algorithm," *Applied Sciences (Switzerland)*, vol. 13, no. 20, Oct. 2023, doi: 10.3390/app132011409.

[10] Y. Tu, F. Tu, Y. Yang, J. Qian, X. Wu, and S. Yang, "Optimization of battery charging and discharging strategies in substation DC systems using the dual self-attention network-N-BEATS model," *Sci. Prog.*, vol. 107, no. 3, Jul. 2024, doi: 10.1177/00368504241274999.

[11] B. Laksahapsoro, M. Bird, S. Acha, and N. Shah, "Optimisation of photovoltaic and battery systems for cost-effective energy solutions in commercial buildings," *Appl. Energy*, vol. 392, Aug. 2025, doi: 10.1016/j.apenergy.2025.125907.

[12] C. Hull, J. Wust, M. J. Booysen, and M. D. McCulloch, "Techno-economic optimization and assessment of solar-battery charging station under grid constraints with varying levels of fleet EV penetration," *Appl. Energy*, vol. 374, Nov. 2024, doi: 10.1016/j.apenergy.2024.123990.

[13] "NASA POWER | Homepage," NASA Prediction of Worldwide Energy Resources (POWER). [Online]. Available: https://power.larc.nasa.gov/(accessed 2024).

[14] G. Zhang *et al.*, "Long life lithium iron phosphate battery and its materials and process," *Energy Storage Science and Technology*, vol. 12, no. 7, p. 2134, Jul. 2023, doi: 10.19799/J.CNKI.2095-4239.2023.0381.

[15] Z. Guo *et al.*, "Characterizing and Visualizing the Impact of Energy Storage on Renewable Energy Curtailment in Bulk Power Systems," *Applied Sciences 2021, Vol. 11, Page 1135*, vol. 11, no. 3, p. 1135, Jan. 2021, doi: 10.3390/APP11031135.

Gia Tue Tang graduated from the Industrial University of Ho Chi Minh City, Vietnam, in 2023 with a B. Eng. degree in Electrical and Electronic Engineering. She is currently pursuing an M.Eng. degree in Electrical Engineering at Ho Chi Minh City University of Technology and Engineering (HCM-UTE), Vietnam. Her areas of research interest are power system stability management.
Email: 2430615@student.hcmute.edu.vn. ORCID: https://orcid.org/0009-0009-2992-3259

Mi Sa Nguyen Thi is a Senior lecturer at the Faculty of Electrical and Electronics Engineering, Ho Chi Minh City University of Technology and Engineering (HCM-UTE), Vietnam. She earned her Ph.D. in Electrical Engineering from National Cheng Kung University (NCKU), Tainan, Taiwan in 2013. Her research interests are simulations of Renewable energy connected to power grid and HVDC.
Email: misa@hcmute.edu.vn. ORCID: https://orcid.org/0009-0008-6597-7492

Phuong Nam Tran received the B.Eng. degree in Electrification and Power Supply from Ho Chi Minh City University of Technology and Engineering (HCM-UTE), Vietnam, in 2003, and the M.Eng. degree in Automation from Ho Chi Minh City University of Transport, Vietnam, in 2009. He is currently pursuing the Ph.D. degree in Electrical Engineering at Ho Chi Minh City University of Technology and Engineering (HCM-UTE), Vietnam. He is also a lecturer at Ho Chi Minh City Vocational College, Vietnam. His research interests include electrical engineering, power systems, automation, and intelligent control systems.
Email: namtp.ncs@hcmute.edu.vn. ORCID: https://orcid.org/0000-0003-2424-2541

Dinh Nhon Truong is an Associate Professor at the Faculty of Electrical and Electronics Engineering, Ho Chi Minh City University of Technology and Engineering (HCM-UTE), Vietnam. He earned his Ph.D. in Electrical Engineering from National Cheng Kung University (NCKU), Tainan, Taiwan. He also serves as the Head of the key Research Team on Sustainable Energy and Applications. His research interests include power system stability, renewable energy conversion systems, microgrids, and FACTS devices.
Email: nhontd@hcmute.edu.vn. ORCID: https://orcid.org/0000-0002-4015-6769